Biosensors and Bioelectronics 51 (2014) 431–436

Contents lists available at ScienceDirect

Biosensors and Bioelectronics

journal homepage: www.elsevier.com/locate/bios

Highly selective detection of microRNA based on distance-dependent electrochemiluminescence resonance energy transfer between CdTe nanocrystals and Au nanoclusters

Yan Cheng, Jianping Lei *, Yunlong Chen, Huangxian Ju

State Key Laboratory of Analytical Chemistry for Life Science, School of Chemistry and Chemical Engineering, Nanjing University, Nanjing 210093, PR China

ARTICLE INFO

Article history:
Received 18 June 2013
Received in revised form
7 August 2013
Accepted 8 August 2013
Available online 17 August 2013

Keywords:
MicroRNA
Electrochemiluminescence resonance energy transfer
Detection
CdTe nanocrystals
Au nanoclusters

ABSTRACT

A distance-dependent electrochemiluminescence resonance energy transfer (ERET) system based on CdTe nanocrystals and Au nanoclusters (Au NCs) was designed with the aid of ligase for highly selective detection of microRNA (miRNA). First, Au NCs functionalized hairpin DNA was synthesized via Au–S chemistry, and characterized with transmission electron microscopy and dynamic light scattering. The resulting hairpin DNA–Au NCs composite can be bound to the carboxylated CdTe nanocrystals via amide reaction on glass carbon electrode. The strong interaction between CdTe nanocrystals and AuNCs led to the electrochemiluminescence (ECL) quenching of CdTe nanocrystals. In the presence of assistant DNA and miRNA, the ligase can selectively ligate both of them on the strand of the hairpin DNA to form long DNA–RNA heteroduplexes. Thus the ECL signal was recovered due to the blocking of the ERET. As a comparison, when directly opening the hairpin DNA by the target, the ECL emission signal is weak owing to the presence of ERET effect at the short distance. Based on the distance-dependent ERET, a 'signal on' ECL system was utilized for the detection of miRNA with the advantages of 6 orders magnitude linear range and excellent sequence specificity. The total detection processing time of the biosensor was approximately 70 min. By substituting the hairpin DNA with different sequences, this strategy as a new signal transduction approach could be conveniently extended for detection of other short miRNA and DNA.

1. Introduction

MicroRNAs (miRNAs) as non-coding RNA with the length of 19–23 nucleotides (Bartel, 2004; He and Hannon, 2004), primarily function as important regulators to regulate fundamental cellular processes through the modulation of gene expression (Cho, 2010; Farh et al., 2005; Feng et al., 2012). So, it is of great significance to develop an accurate, sensitive and low cost miRNA quantification method for biological research and clinical diagnosis. However, several unique characteristics of miRNAs, including the small sizes, sequence homology among family members, and low abundance in total RNA samples, impose restrictions to analyze (Cissell et al., 2007). Some conventional methods (i.e. polymerase chain reaction, Northern blotting, microarrays, etc.) have their individual advantages for the screening of miRNAs (Chapin et al., 2011; Dangwal et al., 2012; Yin et al., 2008), but these techniques are complained on low sensitivity, time and labor consuming. As for hybridization-based detection, it is difficult to label the short probe for selective detection of miRNAs. Therefore, the new strategies focusing on improving the specificity of miRNA profiling measurements are significant and urgent.

In order to address those issues, some emerging strategies such as molecular biological techniques, nanotechnology-based approaches as well as lock nucleic acid (LNA) modified probe are involved in miRNA detection and quantification (Alhasan et al., 2012; Duan et al., 2013; Shen et al., 2013; Wang et al., 2013b; Wen et al., 2012; Yin et al., 2012; Zhu et al., 2013). Especially, the latter has shown great advantages to enable specific identification of highly similar sequences in miRNA family members since the LNA probes show a much higher affinity for their complementary RNAs than conventional RNA- or DNA-based probes (Baker et al., 2012; Ma et al., 2012; Ostergaard and Hrdlicka, 2011). On the other hand, it is an alternative way to enhance the specificity of the detection by elongating the length of the capture probes for improving the melting temperature (T_m), which permits to establish normalized hybridization conditions suitable for all miRNAs (Castoldi et al., 2006; Qavi et al., 2010). Generally, ligase, which is used as an efficient catalyst to form a phosphodiester bond between the juxtaposed 5′-phosphate of the surface-attached single strand DNA (ssDNA) and the 3′-hydroxyl group of unmodified RNA in the presence of a complementary ssDNA

* Corresponding author. Tel./fax: +86 25 83593593.
E-mail address: jpl@nju.edu.cn (J. Lei).

0956-5663/$ - see front matter © 2013 Elsevier B.V. All rights reserved.
http://dx.doi.org/10.1016/j.bios.2013.08.014

template, can ligate two RNAs or RNA/DNA to produce the duplex structure (Lee et al., 2005). In this work, based on the ligation of the T4 RNA Ligase 2, a highly selective detection strategy for miRNA was designed via the distance-dependent electrochemiluminescence (ECL) resonance energy transfer.

ECL is an attractive technique for the sensitive detection of biomolecules due to the separation between the applied voltage and the ECL emission for readout (Richter, 2004). Especially, ECL resonance energy transfer (ERET) has some great potential applications owing to advantages such as its high sensitivity, wide dynamic concentration response range, as well as its potential and spatial controlment (Xu et al., 2011). A series of works were reported by using CdS nanocrystals as ECL donors and Au nanoparticles or $Ru(bpy)_3^{2+}$ as ECL accepts for the detections of DNA, protein and cell in the presence of $K_2S_2O_8$ as coreactant (Wang et al., 2011, 2013a; Wu et al., 2012). Since the rate of energy transfer is highly dependent on the distance between the donor and acceptor (Yun et al., 2005), it is difficult to develop a high sensitivity ERET-based quantification protocol for the short length of miRNA targets. Here, a distance-dependent ECL resonance energy transfer system based on CdTe nanocrystals and Au nanoclusters (NCs) was developed with the aid of ligase by using O_2 as an endogenous coreactant without introduction of exogenous coreactants like $S_2O_8^{2-}$, which was beneficial to the biosensor for detection of miRNA (Scheme 1). First, Au NCs functionalized hairpin DNA was synthesized, which can then be bound to the carboxylated CdTe nanocrystals via amide reaction on glass carbon electrode. When directly opening the hairpin DNA in the presence of target, the ECL emission signal is weak because of the presence of ERET effect between CdTe nanocrystals to Au NCs at the relative short distance. In contrast, in the presence of assistant DNA and miRNA, the ligase can selectively ligate both of them on the strand of the hairpin DNA to form long DNA–RNA heteroduplexes. The long distance should largely increase the ECL signal due to the inhibition of ERET process. Therefore, the proposed ECL biosensor shows an excellent performance of high specificity, 6 orders magnitude linear range and low detection limit down to 21.7 fM. The distance-dependent ERET strategy provides a new concept in the development of high selective microRNA biosensor for gene expression profiling and molecular diagnostics.

2. Materials and methods

2.1. Materials and reagents

T4 RNA ligase 2 was purchased from New England Biolabs Ltd. (Beijing, China). Cadmium chloride ($CdCl_2 \cdot 2.5H_2O$) and meso-2,3-dimercaptosuccinic acid (DMSA) were purchased from Alfa Aesar China Ltd. 6-Mercapto-1-hexanol (MCH) and isopropyl alcohol were purchased from Nanjing chemical reagent Co., Ltd. Tellurium rod (4 mm in diameter) was purchased from Leshan Kayada Photoelectricity Co. (China). Chloroauric acid ($HAuCl_4 \cdot 4H_2O$) was obtained from Shanghai Reagent Co. (Shanghai, China). Glutathione in the reduced form (GSH), tris(hydroxymethyl)aminomethane (Tris), and other chemicals were purchased from Sigma Aldrich without further purification. 0.1 M phosphate buffer salines (PBS) with various pHs were prepared by mixing the stock solutions of 0.1 M NaH_2PO_4 and 0.1 M Na_2HPO_4 containing 0.1 M KNO_3 as the supporting electrolyte. Ultrapure water obtained from a Millipore water purification system ($\geq$ 18 MΩ, Milli-Q, Millipore) was used throughout the work.

The DNA was synthesized by Shanghai Sangon Biotechnology Co. Ltd. (Shanghai, China). All oligonucleotides were purified by using high-performance liquid chromatography and diluted to give stock solutions in 0.1 M Tris–HCl (pH 7.4). The sequences of three oligomers are given as follows:

Hairpin 1: 5′-NH_2-$(CH_2)_6$-GAC T*CG ATA GAT G***CG CCA ATA TTT ACG TGC TGC TAC ACA AAC CAT TAT GTG CTG CTA** *CAT CTA TCG*-$(CH_2)_6$-HS-3′

Hairpin 2: 5′-NH_2-$(CH_2)_6$-GAC T*CG ATA GAT G***CA CAA ACC ATT ATG TGC TGC TA***C ATC TAT CG*-$(CH_2)_6$-HS-3′

Assistant DNA: 5′-phosphate-**TAG CAG CAC GTA AAT ATT GGC G**-3′

All the RNA sequences and diethyprocarbonated (DEPC)-treated water were purchased from Shanghai GenePharma Co., Ltd. (Shanghai, PRC) and purified using high-performance liquid chromatography, which were listed as follows:

Target: 5′-UAGCAGCACAUAAUGGUUUGUG-3′

One-base mismatch: 5′-UAGCAGCACAUAAUGGUUUCUG-3′

Three-base mismatch: 5′-UAACAGCACAAAAUGGUUUCUG-3′

2.2. Apparatus

The synthesis of DMSA-CdTe nanocrystals (i.e. quantum dots, QDs) were carried out using Te rod as working electrode at a CHI 660B. The ECL measurements were carried out on a MPI-E multifunctional electrochemical and chemiluminescent analytical system (Xi'an Remex Analytical Instrument Ltd. Co., China) at room temperature with the photomultiplier tube (PMT, detection range: 300 – 650 nm) as ECL detector biased at 1000 V (Fig. S1). A modified glassy carbon electrode (GCE, 5 mm in diameter, China), platinum wire and Ag/AgCl (saturated KCl) were employed as working, counter and reference electrodes, respectively. Photoluminescence (PL) spectra were obtained on a RF-5301 PC fluorometer (Shimadzu Co., Japan). Transmission electron microscopic (TEM) images were obtained on JEM-2100 (Japan). Dynamic light scattering (DLS)

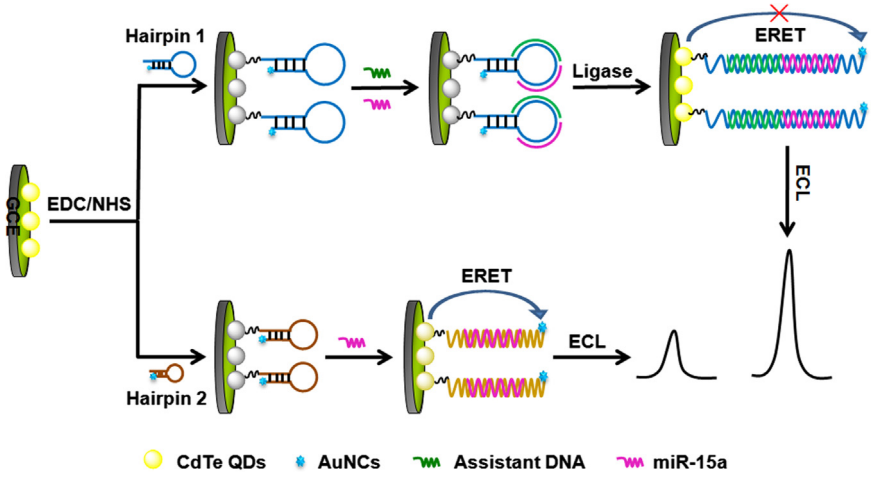

Scheme 1. Schematic illustration of highly selective detection strategy of miRNA based on the distance-dependent ERET between CdTe nanocrystals and Au nanoclusters.

measurement was performed by BI-200SM light scattering apparatus (Brookhaven, U.S.A.).

2.3. Preparation of QDs

The DMSA-CdTe QDs were synthesized according to our electrolysis method (Ge et al., 2008), that is, a green method was employed by using Te rod as working electrode and DMSA as stabilizer under N_2 atmosphere. When a terminal charge quantity of 0.5 C was reached, the resulting solution was refluxed at 80 °C for 20 h to obtain DMSA-CdTe QDs and stored at 4 °C prior to use. According to Peng's empirical equation (Yu et al., 2003), the concentration of the QDs solution was estimated to be 2.7×10^{-6} M from the adsorption peak (Fig. S2).

2.4. Preparation of Au NCs

The Au NCs were prepared according to the previous protocol (Zhou et al., 2010). Briefly, GSH aqueous solution (500 μL, 25 mM) was mixed with 500 μL of $HAuCl_4$ aqueous solution at molar ratio of 1:1, and then kept in dark at room temperature. The color of the solution changed from colorless to pale yellowish after 2 weeks. The solution was first centrifuged at 12,000 *rcf* for 5 min to remove the large nanoparticles. The supernatant was further purified by adding ethanol into the aqueous solution (the ratio between ethanol and water is 1:2). Under this condition, the luminescent Au NCs were precipitated out of the solution while the free GSH and gold ions remained in the solution. The precipitates were then resuspended in aqueous solution and stored at 4 °C.

2.5. Preparation of hairpin DNA/Au NCs composite

The hairpin DNA/Au NCs were prepared via Au–S chemistry (Yun et al., 2005). First, in order to reduce disulfide bonds, 500 μL of 2 μM hairpin DNA in 0.1 M NaCl+0.1 M Tris–HCl buffer (pH 7.4) were activated with 1.5 μL of 10 mM TCEP. Then the activated hairpin DNA was added into 500 μL of Au NCs solution. The resulting colloidal solution was kept in refrigerated at 4 °C over night, and centrifuged at 10,000 *rcf* followed by washing with 0.1 M Tris–HCl buffer, Finally, the resulting hairpin DNA–Au NCs were resuspended in aqueous solution and stored at 4 °C for further use.

2.6. Fabrication of the biosensor

First, the GCE was polished successively with 1.0 and 0.05 μm alumina slurry (Beuhler). After successive sonication in acetone and deionized water, the electrode was dried under N_2. Before modification, QDs solution was mixed with isopropyl alcohol and centrifuged at 8000 *rcf*. The precipitation was washed with a 1:1 mixture of isopropyl alcohol and water, and then dissolved in 20 μL of water and dropped onto GCE. The QDs film on GCE was dried under humid atmosphere at room temperature. The formed QD film was stable due to the low solubility and strong physical absorption of QDs on the surface of GCE. Finally, the CdTe QDs-modified GCE was stored in Tris–HCl buffer (pH 7.4) prior to use.

To activate carboxylic acid group of CdTe QDs, the CdTe QDs modified electrode was immersed in 1 mL of Tris–HCl buffer (pH 7.4) containing 20 mg of EDC and 10 mg of NHS for 1 h at room temperature and then washed with 0.1 M pH 7.4 Tris – HCl solution. 20 μL hairpin DNA–Au NCs was spread on the pre-prepared electrode surface for 20 h in the 100% humidity to obtain the hairpin DNA–Au NCs modified electrode.

2.7. ECL detection

The hairpin DNA–Au NCs modified electrode was incubated with 5′-phosphate-modified assistant DNA and the 3′-hydroxyl group of unlabeled miRNA molecules at 37 °C for 30 min. For the ligation reaction of T4 RNA ligase 2, the resulting electrode

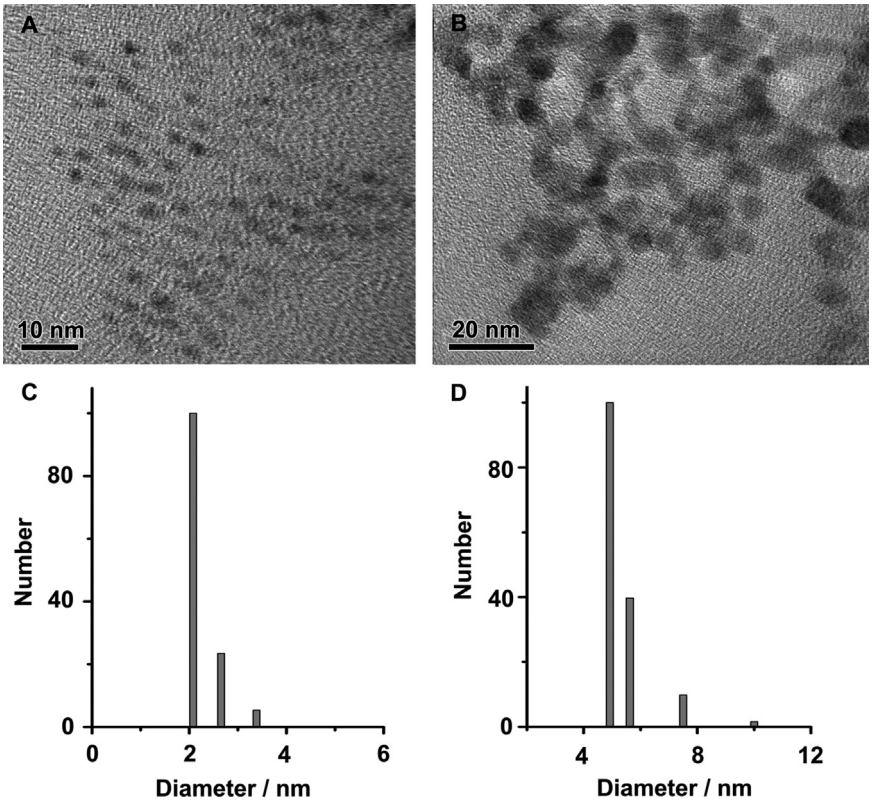

Fig. 1. HRTEM images of (A) Au NCs and (B) CdTe QDs. The hydrodynamic sizes of (C) AuNCs and (D) hairpin DNA–Au NCs composite measured by DLS.

inserted into the reaction mixture for 40 min, in which consisted of T4 RNA ligase 2, PEG 8000, and T4 RNA 2 buffer at a final concentration of 200 U, 25%, and 1 ×, respectively. Finally, the as-prepared biosensor was rinsed three times with deionized water, and then carried out ECL measurements for signal readout in air-saturated PBS. Moreover, no requirement of exhausting air is convenient for the application of the biosensor in practice.

3. Results and discussion

3.1. Characterization of hairpin DNA–Au NCs and CdTe QDs

The topographies and sizes of the obtained CdTe QDs, Au NCs and DNA–Au NCs composite were characterized with high resolution TEM images and DLS pattern in Fig. 1. The typical TEM images of Au NCs (Fig. 1A) and CdTe QDs (Fig. 1B) showed a uniform size distribution of around 1.9 nm and 5 nm, respectively. The dispersibility and stability of the hairpin DNA–Au NCs composite have been evaluated from DLS analysis. This size of Au NCs approximated the mean hydrodynamic diameter of 2.1 nm (Fig. 1C). After the hairpin DNA–Au NCs composite being fabricated, the resulting hydrodynamic diameter is 4.9 nm (Fig. 1D), indicating no massive aggregation of Au NCs and hairpin DNA–Au NCs composite. The increase of hydrodynamic diameter of the hairpin DNA–Au NCs composite indicated that DNA was joined to the Au NCs surface. In addition, the polydispersity index (PDI) of Au NCs and hairpin DNA–Au NCs from the DLS results was also stated to be 0.24 and 0.35, respectively. The small PDI values (PDI < 0.35) indicated the good monodispersity in both cases, which is favorable to construct a uniform sensing platform.

3.2. Performance of the biosensor

In order to confirm the feasibility of the method, ECL-time responses were investigated at the stepwise steps in Fig. 2. The QDs modified electrode had an intensive ECL emission peak at −1.05 V in air-saturated pH 9.0 PBS buffer (curve a). After immobilizing with the hairpin DNA, the ECL intensity slightly decreased (curve b) as a result of the increased impedance and inhibition of O_2 diffusion to the electrode surface. However, there was an outstanding decline of ECL intensity when modifying the hairpin DNA/Au NCs (curve c), which could be attributed to the energy transfer between the excited QDs and Au NCs. Sequentially, when adding the assistant DNA and miRNA, the ECL signal was almost no change in the absence of the ligase. However, in the presence of the ligase, the signal recovered to 78% (curve d), which is contributed to the elongating distance between the QDs and Au NCs after the formation of DNA/miRNA heteroduplexes. In contrast, although the hairpin 2 can be directly opened by target miRNA, the ECL intensity recovered to only about 37.5% (curve e) due to the relatively short distance between the QDs and Au NCs. Therefore, the intensively distance-dependent ERET system between QDs and Au NCs provides a possibility to design a high sensitive and selective method for the detection of miRNA.

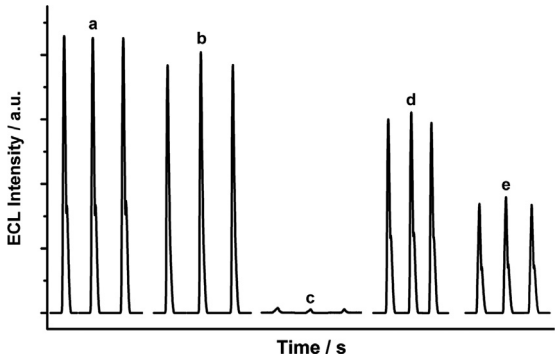

Fig. 2. ECL-time curves of (a) QDs, (b) QDs/hairpin 1 and (c) QDs/hairpin 1–Au NCs modified GCE in air-saturated pH 9.0 PBS. (d) and (e) are ECL responses of QDs/hairpin 1–Au NCs and QDs/hairpin 2–Au NCs modified GCE to 100 nM miRNA in the presence of T4 RNA ligase 2 in air-saturated pH 9.0 PBS buffer, respectively.

3.3. Insights into the quenching mechanism

Generally, the energy transfer efficiency strongly depends on the separation distance between donors and acceptors. To further illuminate quenching mechanism between QDs and Au NCs, fluorescence emission spectra were investigated under different separation distance by using rigid double strand DNA (dsDNA) as the spacer (Fig. 3), in which the QDs and Au NCs are appended at opposite ends via amide reaction and Au–S chemistry, respectively (Fig. S3). For the dsDNA with 44 mer and 22 mer without regarding single strand DNA spacer, the separation distances can be calculated to be 14.96 nm and 7.48 nm, respectively (Li et al., 2011; Jennings et al., 2006). As a result, the quenching of fluorescence emission of QDs was obviously observed at 475 nm (curve b), which should be attributed to Förster resonance energy transfer (FRET) from the QDs to Au NCs at the short distance less 10 nm. In contrast, at the relative long distance (14.96 nm) after ligation reaction, a fluorescence quenching of QDs became weak (curve a). This phenomenon can be explained by surface energy transfer between the QDs to the Au NCs (Yun et al., 2005), in which is energy transfer from a dipole to a metallic surface with the detectable distance limited to < 20 nm (Singh and Strouse, 2010). The different quenching efficiencies can provide a detectable ECL signal for the determination of miRNA. Moreover, due to the small size, this reported QDs/Au nanoclusters ECL system showed more efficient ECL quenching effect comparing with gold or silver nanoparticles, leading to a highly sensitive ECL strategy for miRNA detection.

3.4. Optimization of conditions for ECL detection

To efficiently apply the ERET system in miRNA detection, several experimental parameters including the pH value, concentrations of the T4 RNA ligase 2, incubation time of the hybridization and the time of ligation reaction were optimized (Fig. 4). The ECL intensity increased with the increasing pH of detection solution from 6.0 to 10.0 (Fig. 4A) because the electrogenerated intermediates (e.g. $O_2^{\bullet-}$ and $HO^{\bullet}$) of dissolved O_2 as well as the resulting H_2O_2 as the coreactant were more stable at high pH. Considering that pH 9.0 was favorable for bioanalysis applications, 0.1 M pH 9.0 PBS

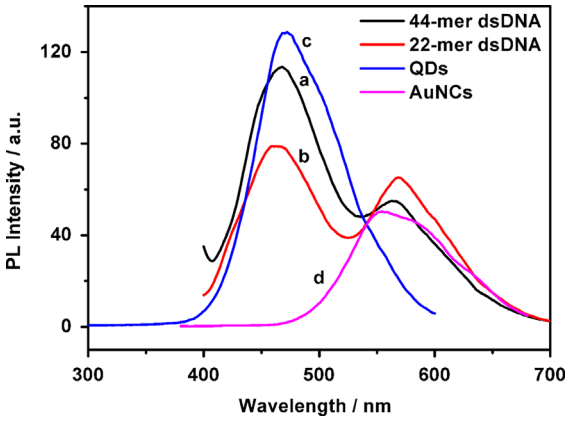

Fig. 3. Fluorescence emission spectral of QDs–dsDNA–AuNCs conjugate with 44 base pairs (a) and 22 base pairs (b), QDs (c) and AuNCs (d).

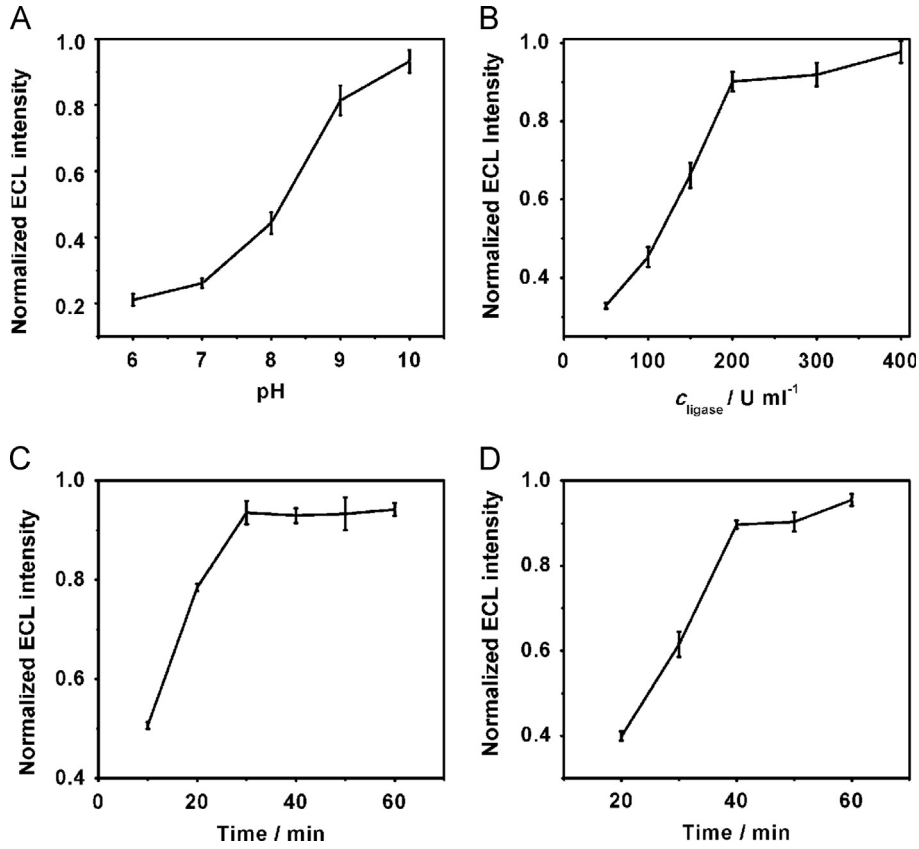

Fig. 4. Effects of (A) the pH, (B) concentrations of T4 RNA ligase 2, (C) incubation time of the hybridization, and (D) the time of ligation reaction on normalized ECL intensity at 1 μM of hairpin 1, 100 nM of assistant DNA and 100 nM of miRNA in air-saturated PBS buffer containing 0.1 M KNO_3. When one parameter changes the others are under their optimal conditions.

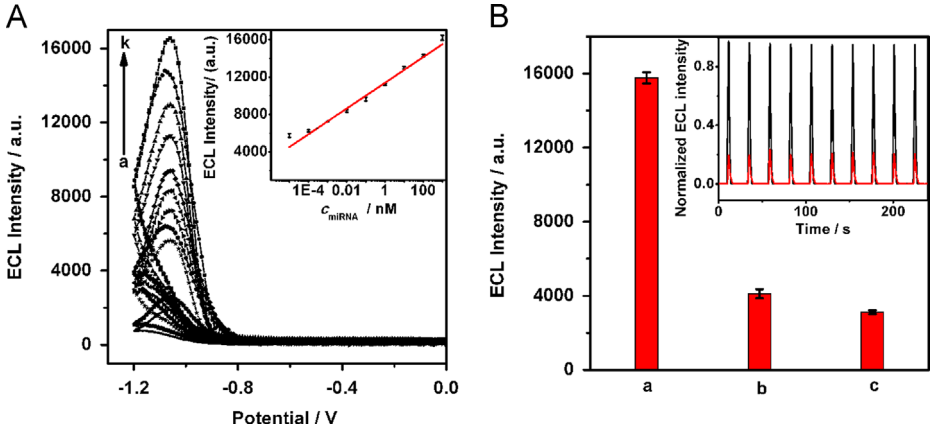

Fig. 5. (A) ECL responses of the biosensor to 0, 1×10^{-6}, 1×10^{-5}, 1×10^{-4}, 1×10^{-3}, 0.01, 0.1, 1, 10, 100 and 1000 nM of miRNA (from *a* to *k*) in air-saturated pH 9.0 PBS buffer. Inset: Linear calibration plot for miRNA detection. (B) The ECL intensity for detection of 100 nM complementary target (a), single-base mismatched strand (b), and three-base mismatched strand (c). Inset: Continuous cyclic scans of GCE/QDs/hairpin 1–Au NCs (red) and then incubation with miRNA in the presence of 100 nM of assistant DNA and T4 RNA ligase 2 (black) in air-saturated pH 9.0 PBS buffer. Scan rate: 0.1 V s^{-1}. (For interpretation of the references to color in this figure legend, the reader is referred to the web version of this article.)

buffer was used throughout the following experiments. On the other hand, the detection sensitivity depended on the formation of the duplex of DNA and miRNA via ligation reaction by ligase on the electrode surface. Thus the hybridization time of among hairpin DNA, assistant DNA and the target, the time of the ligation reaction and concentrations of T4 RNA ligase 2 are important in this method. As shown in Fig. 4B, the ECL peak intensity had no obvious change after concentrations of T4 RNA ligase 2 reached the 200 U/mL, indicating that the ligase was sufficient for specific conjugation of assistant DNA and miRNA. Thus, the 200 U/mL of T4 RNA ligase 2 was chosen in the ECL detection. In addition, the hybridization time and the time of ligation reaction were chosen to be 30 min and 40 min (Fig. 4C and D), respectively, in which the ECL intensity reached a platform, and can efficiently facilitate the detection.

3.5. Quantitative measurement

Above results revealed that the ERET upon the introduction of hairpin DNA–Au NCs bioconjugates and ligase could effectively amplify the sensing signal and improve the detection sensitivity.

Thus the distance-dependent ERET method was applied for the quantitative measurement of miRNA. As shown in Fig. 5A, the cathodic ECL peak intensity around −1.05 V increased with the increasing of concentrations of miRNA from 1 fM to1 μM. A linear relationship between miRNA concentration and ECL intensity was plotted in the concentration range of 100 fM to 100 nM with a correlation coefficient of 0.993 (inset of Fig. 5A). Meanwhile, miRNA could be detected at a limit of detection (LOD) of 21.7 fM at signal to noise ratio $S/N=3$ without any separation or amplification step. Compared with other methods (Table S1), the designed biosensor showed wide detectable concentration range and low LOD. The low detection limit of this biosensor can be attributed to the high affinity and specificity of the ligase as well as the low background noise inherent in ECL detection.

3.6. Selectivity and stability of biosensor

The selectivity of the ERET-based miRNA biosensor was investigated by measuring the ECL response of the proposed biosensor to three types of miRNA sequences at the same concentration (100 nM), including complementary target, single-base mismatched strand, and three-base mismatched strand in the same condition. As shown in Fig. 5B, the proposed system displayed high fidelity in discriminating perfectly complementary target and the mismatched stands. The ECL intensity of perfectly complementary target was 3.9 times of that for single-base mismatch sequence, and the response to the three-base mismatch strand was only 19% of that for the perfectly complementary target. The high sequence specificity may be attributed to the high affinity and unique specificity of the ligase (Tyagi and Kramer, 1996). These results suggested that this detection approach had high sequence specificity and potential application in the short ssDNA analysis.

The proposed biosensor showed stable ECL signal of quenching (inset of Fig. 5B, red curve) and recovering response (inset of Fig. 5B, black curve) upon consecutive potential scans, indicating the feasibility for ECL detection. The relative standard deviation (RSD) for ten parallel measurements at GCE/QDs/hairpin 1–Au NCs without and with ligation reaction were 1.12% and 0.93%, respectively, indicating a good precision. The detection 100 nM of miRNA at three independent electrodes showed a RSD of 0.98%, giving an acceptable fabrication reproducibility. When the sensor was not in use, it was stored in air condition at room temperature and measured in pH 9.0 PBS every few days. No obvious change in the ECL intensity was observed after storage for 4 weeks, exhibiting a potential application in practice.

4. Conclusions

The distance-dependent ECL resonance energy transfer system based on CdTe nanocrystals to Au nanoclusters was successfully constructed with the aid of ligase for detection of miRNA. Compared to the method that the short hairpin DNA was directly opened by miRNA, this system integrated with the ligation reaction to form long DNA–RNA heteroduplexes, and thus the ECL signal was significantly recovered due to the blocking of the ERET. Also, this strategy demonstrated great advantages in sensitivity and selectivity due to the high affinity and specificity of the ligase as well as the low background noise inherent in ECL detection. Using this ERET system, miRNA could be detected with the 6 orders of magnitude linear relationship and a detection limit at femtomolar level without any separation and amplification step. In addition, high specificity can be achieved to clearly discriminate one-base mismatched miRNA. Associated with the advantages of ECL rapid detection and low-cost, the proposed strategy provided a convenient tool and signal transduction platform for the specific analysis of miRNA in the related miRNA family members.

Acknowledgments

This work was financially supported by the National Basic Research Program of China (2010CB732400), National Natural Science Foundation of China (21075060, 21135002, 21121091), and the program for New Century Excellent Talents in University (NCET100479).

Appendix A. Supporting information

Supplementary data associated with this article can be found in the online version at http://dx.doi.org/10.1016/j.bios.2013.08.014.

References

Alhasan, A.H., Kim, D.Y., Daniel, W.L., Watson, E., Meeks, J.J., Thaxton, C.S., Mirkin, C. A., 2012. Analytical Chemistry 84, 4153–4160.
Baker, M.B., Bao, G., Searles, C.D., 2012. Nucleic Acids Research 40, e13.
Bartel, D.P., 2004. Cell 116, 281–297.
Castoldi, M., Schmidt, S., Benes, V., Noerholm, M., Kulozik, A.E., Hentze, M.W., Muckenthaler, M.U., 2006. RNA 12, 913–920.
Chapin, S.C., Appleyard, D.C., Pregibon, D.C., Doyle, P.S., 2011. Angewandte Chemie International Edition 50, 2289–2293.
Cho, W.C., 2010. Biochimica et Biophysica Acta 1805, 209–217.
Cissell, K.A., Shrestha, S., Deo, S.K., 2007. Analytical Chemistry 79, 4754–4761.
Dangwal, S., Bang, C., Thum, T., 2012. Cardiovascular Research 93, 545–554.
Duan, R.X., Zuo, X.L., Wang, S.T., Quan, X.Y., Chen, D.L., Chen, Z.F., Jiang, L., Fan, C.H., Xia, F., 2013. Journal of American Chemical Society 135, 4604–4607.
Farh, K.K., Grimson, A., Jan, C., Lewis, B.P., Johnston, W.K., Lim, L.P., Burge, C.B., Bartel, D.P., 2005. Science 310, 1817–1821.
Feng, M.J., Shi, F., Qiu, C., Peng, W.K., 2012. International Immunopharmacology 13, 347–353.
Ge, C.W., Xu, M., Liu, J., Lei, J.P., Ju, H.X., 2008. Chemical Communications 4, 450–452.
He, L., Hannon, G.J., 2004. Nature Reviews Genetics 5, 522–531.
Jennings, T.L., Singh, M.P., Strouse, G.F., 2006. Journal of American Chemical Society 128, 5462–5467.
Lee, H.J., Wark, A.W., Li, Y., Corn, R.M., 2005. Analytical Chemistry 77, 7832–7837.
Li, M., Cushing, S.K., Wang, Q., Shi, X., Hornak, L.A., Hong, Z., Wu, N., 2011. Journal of Physical Chemistry Letters 2, 2125–2129.
Ma, C.B., Yeung, E.S., Qi, S.D., Han, R., 2012. Analytical and Bioanalytical Chemistry 402, 2217–2220.
Ostergaard, M.E., Hrdlicka, P.J., 2011. Chemical Society Reviews 40, 5771–5788.
Qavi, A.J., Kindt, J.T., Bailey, R.C., 2010. Analytical and Bioanalytical Chemistry 398, 2535–2549.
Richter, M.M., 2004. Chemical Reviews 104, 3003–3036.
Shen, W., Deng, H.M., Ren, Y.Q., Gao, Z.Q., 2013. Biosensors and Bioelectronics 44, 171–176.
Tyagi, S., Kramer, F.R., 1996. Nature Nanotechnology 14, 303–308.
Singh, M.P., Strouse, G.F., 2010. Journal of American Chemical Society 132, 9383–9391.
Wang, J., Shan, Y., Zhao, W.W., Xu, J.J., Chen, H.Y., 2011. Analytical Chemistry 83, 4004–4011.
Wang, J., Zhao, W.W., Zhou, H., Xu, J.J., Chen, H.Y., 2013a. Biosensors and Bioelectronics 41, 615–620.
Wang, X.P., Yin, B.C., Wang, P., Ye, B.C., 2013b. Biosensors and Bioelectronics 42, 131–135.
Wen, Y.L., Pei, H., Shen, Y., Xi, J.J., Lin, M.H., Lu, N., Shen, X.Z., Li, J., Fan, C.H., 2012. Scientific Reports 2, 867.
Wu, M.S., Shi, H.W., He, L.J., Xu, J.J., Chen, H.Y., 2012. Analytical Chemistry 84, 4207–4213.
Xu, S.J., Liu, Y., Wang, T.H., Li, J.H., 2011. Analytical Chemistry 83, 3817–3823.
Yin, H.S., Zhou, Y.L., Zhang, H.X., Meng, X.M., Ai, S.Y., 2012. Biosensors and Bioelectronics 33, 247–253.
Yin, J.Q., Zhao, R.C., Morris, K.V., 2008. Trends in Biotechnology 26, 70–76.
Yu, W.W., Qu, L.H., Guo, W.Z., Peng, X.G., 2003. Chemistry of Materials 15, 2854–2860.
Yun, C.S., Javier, A., Jennings, T., Fisher, M., Hira, S., Peterson, S., Hopkins, B., Reich, N.O., Strouse, G.F., 2005. Journal of American Chemical Society 127, 3115–3119.
Zhou, C., Sun, C., Yu, M.X., Qin, Y.P., Wang, J.G., Kim, M., Zheng, J., 2010. Journal of Physical Chemistry C 114, 7727–7732.
Zhu, X., Zhou, X.M, Xing, D., 2013. Chemistry—A European Journal 19, 5487–5494.